

Nonlinear Optical Effects in the LIGO Gravitational-wave Interferometer

Phil Willems

LIGO Project, California Institute of Technology, Mail Stop 18-34, Pasadena CA 91125 USA

ABSTRACT

LIGO (Laser Interferometer Gravitational-wave Observatory) is a trio of sensitive Michelson interferometers designed to detect extremely relativistic astrophysical processes by the ripples they produce in spacetime. For best sensitivity, these interferometers are kilometers long, contain nearly unstable cavities, and operate at high optical power, making them uniquely susceptible to thermal aberrations and radiation-pressure-derived instabilities. We describe the LIGO interferometers, and their high power lasers and input optics, and described how thermal aberrations have been successfully controlled using adaptive corrective heating. The Advanced LIGO detectors, an upgrade to LIGO planned for installation in the year 2010, will operate with even higher optical power. We detail the additional challenges in construction and thermal compensation for Advanced LIGO, and detail how radiation-pressure derived instabilities influence the design, operation, and sensitivity of Advanced LIGO.

Keywords: gravitational waves, thermal lensing, lasers, instability, radiation pressure, quantum noise

1. INTRODUCTION

Einstein's General Theory of Relativity predicts the existence of gravitational waves¹, ripples in spacetime that travel at the speed of light, inducing an oscillating quadrupolar strain in space. The LIGO Project² is a trio of Michelson interferometers designed to detect astrophysical gravitational waves. To make the strain of spacetime detectably large, the interferometer arms are 4 kilometers long, and the light storage time is increased by the use of input mirrors that turn the arms into Fabry-Perot cavities. The interferometers are operated on a dark fringe, so that a passing gravitational wave is signaled by light leaking to the output from the differentially modulated arms. To reduce the shot noise of the detector, LIGO increases the stored light power by recycling the light reflected from the interferometer to the input laser with an input power recycling mirror, thus rendering the whole interferometer a Fabry-Perot cavity. The gravitational waves generate optical sidebands at audio frequencies, which are detected by heterodyning them against RF sidebands resonating in the same interferometer everywhere except in the arms.

Displacement sensitivity of the order of 10^{-19} m/ $\sqrt{\text{Hz}}$ is required for reasonable rates of gravitational wave detection. Therefore, any motion of the mirror surfaces must be suppressed below this level. For this reason, the interferometer mirrors are suspended from metal wire loops on isolation platforms to attenuate seismic excitation, and housed in vacuum to prevent acoustic excitation, air currents, and refractive phase noise. At the frequency range of maximum sensitivity (~ 100 Hz), the displacement sensitivity is limited by irreducible thermal motion within the mirrors themselves and photon shot noise. The sensitivities of the three detectors during LIGO's fourth science run (February 22 until March 23, 2005) are shown in Figure 1.

Strain Sensivities for the LIGO Interferometers

Best Performance for S4 LIGO-G050230-02-E

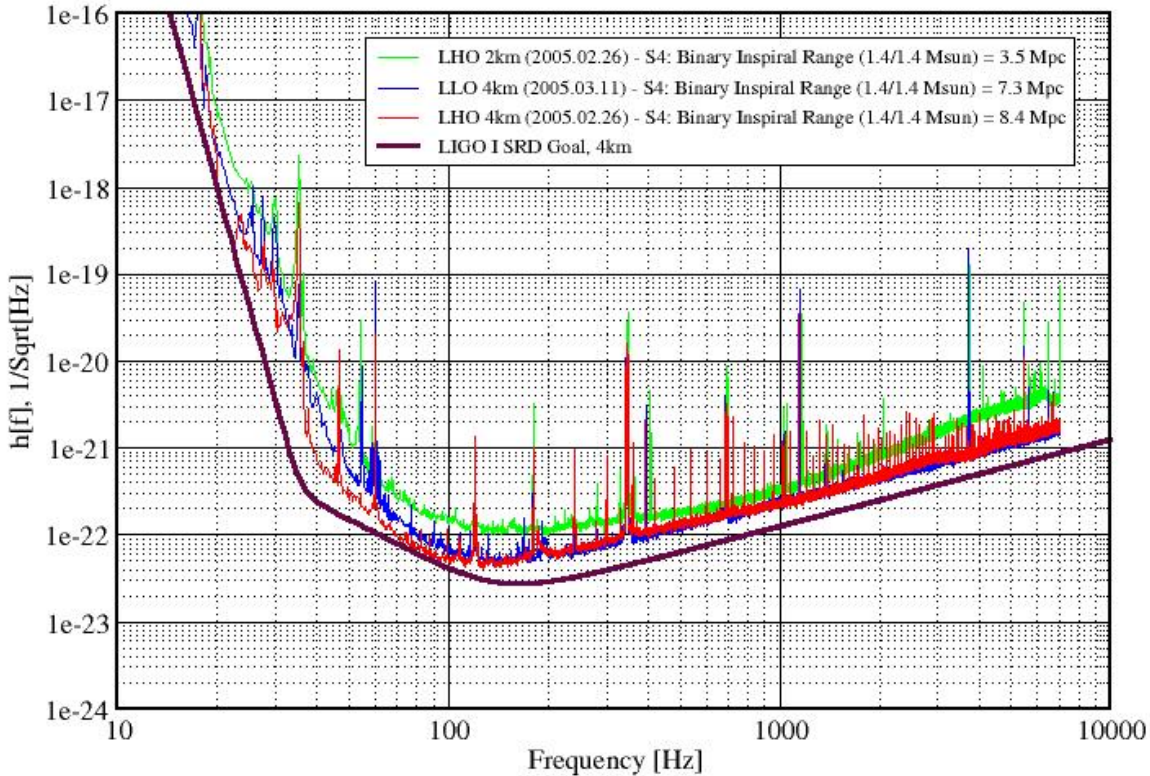


Figure 1: Best strain sensitivities of the LIGO interferometers during their 4th science run.

1.1. Input optics

The optical power used in LIGO is not very large by current standards, but the stability and mode quality requirements are extremely stringent and worth discussing in some detail.

1.1.1. The laser

LIGO is designed to operate with 6W of optical input to the power recycling mirror. This is provided by a 10W Nd:YAG laser in a MOPA configuration with an NPRO injector. The choice of Nd:YAG lasers over other types was based upon their high reliability, relative ease of stabilization, and scalability to higher powers for future upgrades to the LIGO Project. The extreme displacement sensitivity of LIGO places high demands on the frequency and intensity stability, mode shape, and jitter of the laser beam. Frequency noise couples directly through the interferometer due to an asymmetry of the arm lengths and reflectivities and becomes indistinguishable from signal at the output. Intensity noise leads to a differential radiation pressure on the arm mirrors due to unavoidable imbalances in the arm power gains, which then leads to differential arm motion and noise at the output. The beam quality and jitter are improved by passing the light through a fixed spacer cavity pre-modecleaner locked to the laser output frequency, followed by a suspended 12-m modecleaner after the optical heterodyne sidebands are added. The amplitude is stabilized by sampling a pickoff beam after the pre-mode cleaner and feeding back to the current of the pump laser diodes in the power amplifier of the MOPA. Provisions have been made for sampling the intensity after the suspended 12-m mode cleaner, which could potentially introduce amplitude modulation as a consequence of the frequency stabilization it performs, but in practice this has not yet been necessary.

The frequency stabilization is more complex, as the free-running laser frequency noise must be suppressed by up to nine orders of magnitude within the LIGO bandwidth. Internally, the frequency of the laser is controlled using a slow actuator based on thermo-electric tuning of the NPRO temperature, a fast actuator based on a PZT attached to the NPRO crystal, and a phase-correcting EOM between the master oscillator and power amplifier. Externally, the laser frequency is first stabilized against a thermally controlled reference cavity. At intermediate frequencies the LIGO interferometer itself is the most stable reference available, and the common mode arm length signal is used to stabilize the suspended mode cleaner, which in turn is used to stabilize the laser frequency. Over very long times (hours), the frequency must be allowed to drift to follow the expansion and contraction of the arm cavities during long lock periods due to the Earth's tides stretching the ground between the mirrors. A 'tidal servo' adjusts the temperature of the reference cavity to track the differential change in the arm length.

1.1.2. The modulators

The cavity lengths in LIGO are sensed by heterodyning the main interferometer beam with RF phase-modulated sidebands using a Pound-Drever-Hall scheme³. Because the main, or carrier, beam resonates in all cavities of the interferometer, but the various RF sidebands resonate only in some or no cavities, mirror motions will differentially phase-modulate the different beams, and thereby be sensed in a demodulated heterodyne output. LIGO requires three pairs of RF sidebands: one pair resonates in the recycling cavity for GW detection and Michelson and arm cavity control, one pair resonates in the mode cleaner but not the recycling cavity for recycling cavity control, and one pair is rejected from the suspended mode cleaner for control of the suspended mode cleaner (see Figure 2).

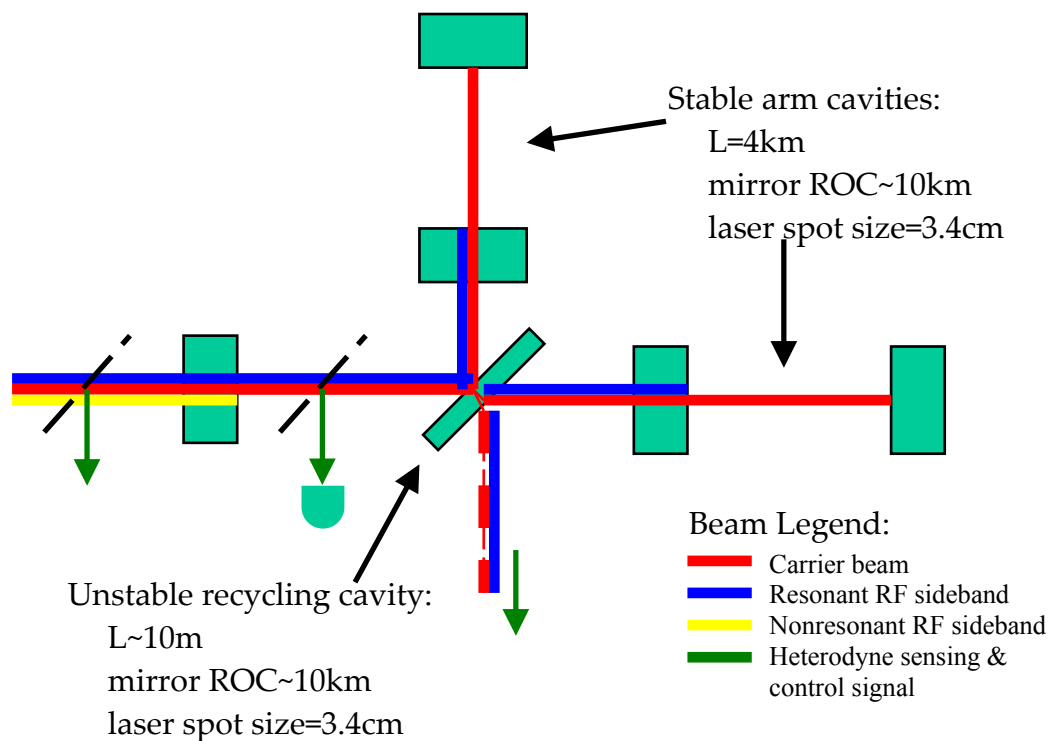


Figure 2: RF heterodyne resonance conditions. The suspended mode cleaner and RF sideband dedicated to its control are not shown.

These sidebands are generated by three sequential New Focus 4003 LiNbO₃ phase modulators. Intermodulation sidebands are produced in this configuration but do not affect the interferometer control. These modulators are robust at 10W input power but produce a 3.3m thermal lens which must be corrected with lenses before being input to the suspended mode cleaner.

1.1.3. The suspended mode cleaner

The suspended mode cleaner serves several purposes: it strips non-TEM00 light from the interferometer beam; it filters amplitude and frequency noise from the beam; it suppresses beam jitter; and it provides a feedback signal for frequency stabilization. To serve these functions to the level required for LIGO sensitivity, the finesse of this cavity is rather large at ~ 1450 , and the mirrors are suspended for low displacement noise. The large circulating power reflecting off such weakly mounted optics in a sensitive cavity renders the radiation pressure force on the mirrors observable. Figure 3 shows the difference in the average position of one of the mode cleaner mirrors as the cavity falls into and out of lock.

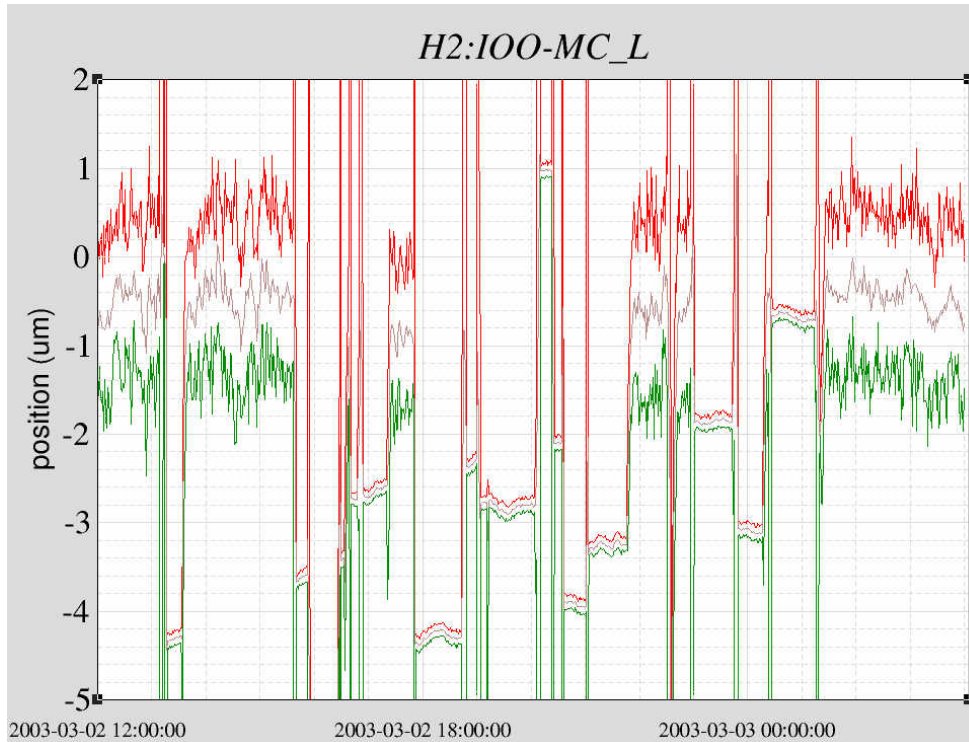


Figure 3: Radiation pressure is observable in the offset between the lower, locked mode cleaner states and the noisier upper, unlocked states. The red, green, and grey curves show the maximum, minimum, and mean mirror displacement per time sample in the interferometer data stream, and the abscissa shows day and time of measurement.

For LIGO, the radiation pressure produces only slight offsets in the mirror positions that can be compensated using servos. In the higher power of Advanced LIGO, to be discussed later, radiation pressure will be sufficiently strong to dynamically nonlinearize the cavity response and interferometer quantum sensitivity through mirror displacement.

1.1.4. The Faraday isolator

The power recycling mirror does not completely store the input light in the interferometer- a small fraction of the light is reflected for length sensing purposes³. The Faraday isolator that protects the laser from this reflected light is located after the suspended mode cleaner. Using a TGG crystal, at 10W input power the isolation is better than 35dB, the through polarization is better than 100:1, and the optical loss is 8%. The thermal lens has about 100m focal length at full throughput power, which is tolerable. The diverted beam is used as the pickoff signal for interferometer length control.

1.2. Thermal aberrations

Optical power absorbed in the input test masses creates a thermal gradient in the optic substrate, creating thermal aberrations in the power recycling cavity through the thermo-optic effect. To understand the effects of thermal aberrations in the main interferometer optics, it is necessary to understand the method used to control the mirror spacing. We refer to Figure 2. At several points in the interferometer, the resonating light is picked off and read by a photodetector, and the optical heterodyne signal between the main beam and RF sidebands is demodulated and fed back to the mirror positions. This same technique with quadrant photodetectors is used to sense and control the mirror orientations⁴. Good overlap between the main (or *carrier*) and sideband beams profiles is essential to this technique, and the good profile of the carrier, which contains the gravitational wave signal, is of highest importance.

The kilometer-scale arm cavities are stable, with a mode spot size of 3.4cm. It is desirable that the arm cavity mode resonate in the power recycling cavity regardless of the level of thermal aberration. How this is done is as follows: the recycling cavity is made marginally stable, so that all transverse modes have equal Guoy phases and resonate at the same time. The recycling cavity length is then set so that all modes are exactly antiresonant (phase shift of π round trip) in the absence of the arm cavity (for example, when the end mirror is misaligned). The arm cavity input reflectivity and internal loss are such that the amplitude reflection coefficient for light resonant in the cavity is -1. Such a cavity is said to be overcoupled. This amplitude reflection coefficient of -1 in turn makes the power recycling cavity resonant, *but only for the mode that resonates in the arm cavity*. Thus, only the TEM00 mode can resonate in the power recycling cavity because only that mode resonates in the arm.

The story is different for the RF sidebands. The free spectral range of the power recycling cavity is twice the sideband frequency for one of the RF sideband pairs, so that pair resonates there without resonating in the arms. However, in this case all its transverse modes are equally resonant and the resonating field is very sensitive to small aberrations, the typical condition for marginally stable cavities. The price for very clean carrier modes is distorted RF sideband modes.

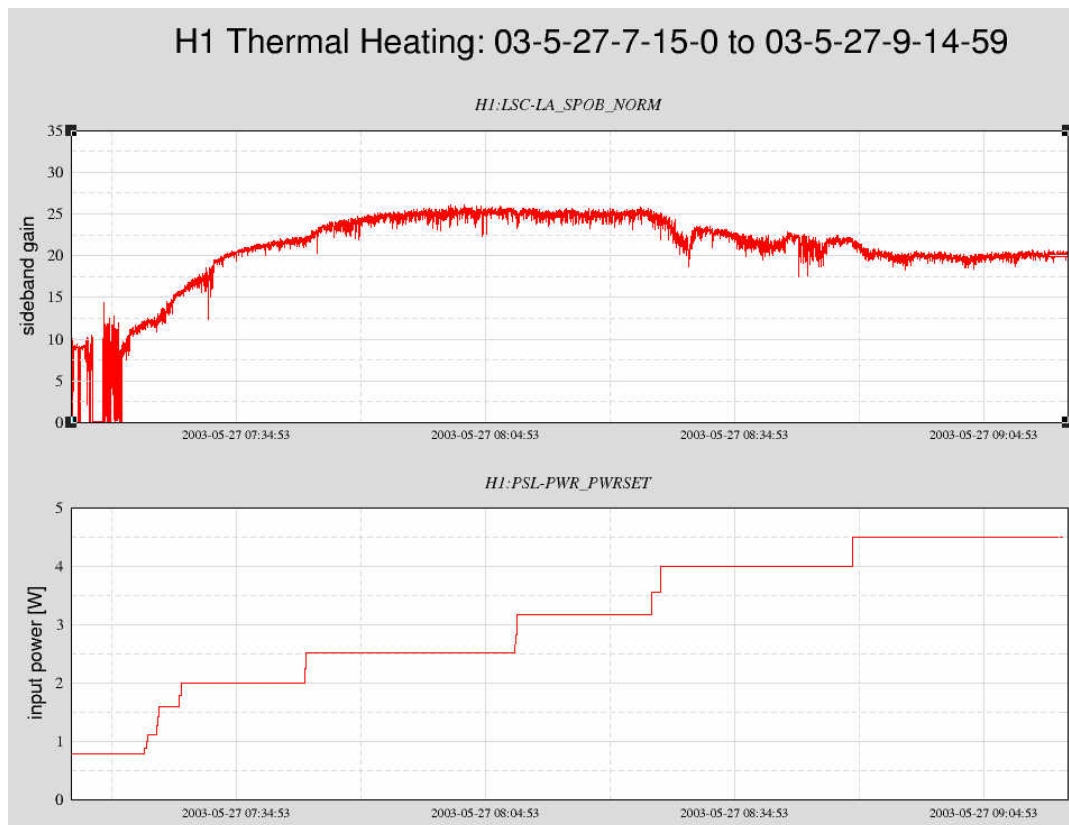


Figure 4: Saturation of the RF sideband power inside the recycling cavity as the input laser power is increased. The lower curve shows the optical power input to the power recycling cavity, while the upper curve shows the stored RF

sideband power. Thermal aberration is the cause of the saturation at 2.5 W input, and of the slow drift in the RF power after the input is varied.

Since distorted RF sidebands are still detrimental, we attempted to design the optics with radii of curvature such that the heating at full laser power would distort the optics into optimal alignment. As Figure 4 shows, this approach was not entirely successful, because we were not successful in predicting the actual heating of the optics *in situ* before polishing the mirror surfaces. In one of the interferometers, rather than reaching the maximum RF sideband gain at full power, the sideband power saturates at 2.5W- this interferometer is overheating. The other two interferometers also had suboptimal mirror radii of curvature, though to a lesser degree.

We retrofitted a carbon dioxide laser projector onto the system to irradiate the input test masses with a heating pattern that could heat either the center of the optic (mimicking self-absorption, for aligned operation and diagnostics at low power) or on an annulus around the center of the optic to even the heat distribution in the case of overheating. Figure 5 shows how the central heating feature allows us to smoothly control the size of the RF sideband beam resonating in the power recycling cavity and thus optimize the overlap with the carrier beam. With this addition, and replacement of one strongly absorbing optic, it is now possible to run all three interferometers at their full design power of 6W input.

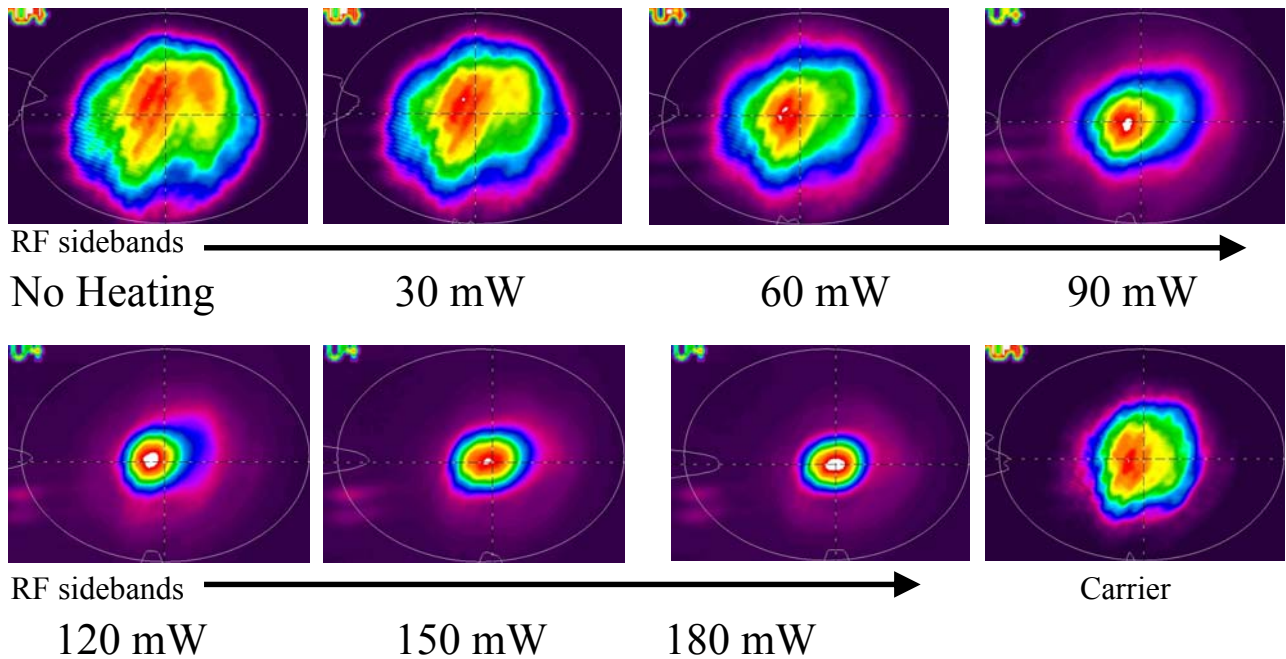


Figure 5: Mode overlap between RF sidebands and carrier vs. thermal compensation power. The overlap is optimized at 90mW heating power.

2. Advanced LIGO

A proposed upgrade to LIGO- called Advanced LIGO- is planned for installation starting in 2010⁵. Its goal is to improve the sensitivity of the interferometer by a factor of ten or better over the full detector bandwidth. To do this it will incorporate many new features: the passive seismic isolation will be replaced by active isolation⁶, and the simple mirror pendulums will be replaced with quadruple mirror pendulums⁷; the steel suspension wires will be replaced by fused silica suspension wires with lower thermal noise⁷; the 10kg mirrors will be replaced with 40kg mirrors for less recoil from radiation pressure; and the input laser power will increase from 6W to 120W. Finally, the optical configuration will include another suspended mirror at the output of the interferometer, called the signal recycling mirror, whose function is to tailor the output transfer function of the gravitational wave sidebands from the interferometer, increasing sensitivity at frequencies from 200-1000Hz⁸.

2.1. Advanced LIGO high power laser

The 120W optical power input to Advanced LIGO will come from a 180W Nd:YAG MOPA laser provided by Laser Zentrum Hannover. A description of this laser will be reported in another article.

2.2. Advanced LIGO input optics

The large increase in optical power will place great strains on the input optics. The thermal lensing in the modulators and isolators, tolerable in LIGO, becomes unacceptably large in Advanced LIGO.

The addition of the signal recycling mirror obliges Advanced LIGO to introduce a fourth RF sideband for interferometer control, and a different feedback topology. These changes now make the intermodulation product sidebands produced by sequential modulators unacceptable, since they interfere with control signals produced in the interferometer. For this reason the input optics will include a Mach-Zehnder with phase modulators placed in separate arms to prevent intermodulation. LiNiO₃ modulators have been shown to have severe, position-dependent thermal lensing at 30W through power, so in Advanced LIGO new crystals must be used. We have found RTA and RTP to both have negligible thermal lensing at 95W through power, with RFAM characteristics no worse than the levels seen in LIGO's LiNiO₃ crystals.

The Faraday isolator in Advanced LIGO will continue to use TGG, but the thermal lensing at 120W through power will require compensation. A scheme for passive thermal compensation using a negative dn/dT material in series with the isolator has been demonstrated⁹ and is reported in a companion article to this one¹⁰.

2.3. Thermal Aberrations

The stored arm power will increase from 15kW in LIGO to 850kW in Advanced LIGO, making the thermal aberrations much more severe, and their manifestations more numerous. If the marginally stable recycling cavity design is chosen again for Advanced LIGO (as is the current design), the distortion of the RF sidebands will be an even bigger issue than in initial LIGO. However, Advanced LIGO is planned to use a DC homodyne readout scheme for the gravitational wave sidebands at the output port. This reduces the importance of RF sideband aberrations. They are still needed for control of the other interferometer degrees of freedom, and the requirement is that the RF sidebands not saturate for even the highest input power.

In the high power of Advanced LIGO, even the arm cavities will see significant distortion, through thermoelastic expansion of the mirrors' high-reflectance surfaces. Assuming the absorption in the substrates and coatings to be homogeneous, self-heating will lead to a thermoelastic 'bump' in the center of the mirror, increasing the radius of curvature and changing the spot size by some tens of percent at maximum optical power. If any point absorbers are present on the coating, these will cause 'thermal microroughness', small-scale blisters on the optic surface that scatter power from the arm. The high finesse required in the arm cavities sets an upper limit on the optical scatter from the arms, and thereby on the allowable size and number of coating point absorbers.

By far the most serious thermal effect is the aberration of the gravitational wave sidebands as they pass through the signal recycling cavity. These sidebands, generated in the arms by the passing gravitational wave, will be converted from the fundamental Gaussian mode to higher-order transverse modes having reduced overlap with the carrier. This can be considered as a loss of power in the signal cavity, and directly reduces the sensitivity of the detector. Figure 6 shows how the signal losses affect how far in megaparsecs we can see an inspiral of a binary neutron star system.

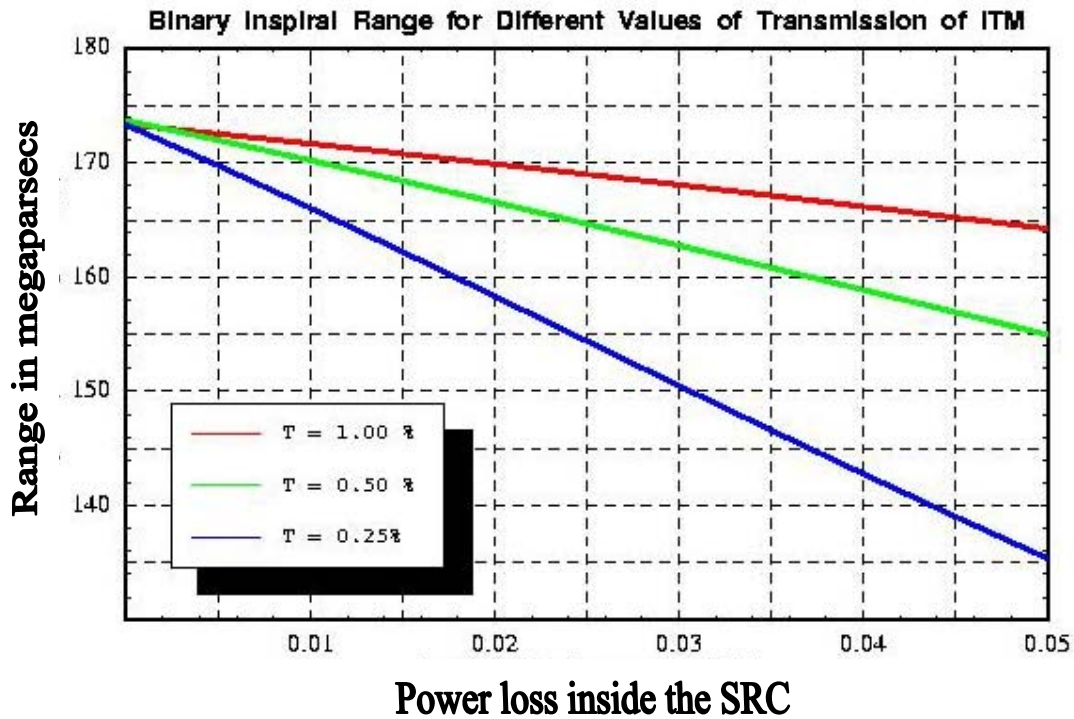


Figure 6: Dependence of Advanced LIGO astronomical reach to binary neutron star inspirals as a function of signal cavity loss, based upon a detection SNR of 8. The different curves correspond to different arm cavity input mirror transmittances.

Thermal compensation is incorporated into the design Advanced LIGO from the outset. The compensation will be applied to fused silica plates suspended immediately in front of the arm cavity input mirrors inside the recycling cavity—this will prevent noise in the thermal actuators from being applied to the input mirrors, which can directly couple to the very sensitive arm cavities. Two types of actuator will be used. Incandescent ring heaters suspended in the vacuum near the compensation plates will apply an axisymmetric compensation that should be close to ideal for homogeneous coating or substrate absorption in the arm cavity input mirrors. Carbon dioxide laser heat projectors, as in initial LIGO, will be projected onto the compensation plates from outside the vacuum to refine the heating pattern. Both these types of actuators have been tested in tabletop experiments^{11,12}.

Initial LIGO has no sensors on the test masses to measure the thermal aberrations. Advanced LIGO will have dedicated wavefront sensors on each arm cavity input mirror to provide feedback to the thermal compensators. These will be either Hartmann sensors or white light phase modulated Fizeau interferometers as recently demonstrated at the Institute for Applied Physics in Nizhny Novgorod¹³.

2.4. Radiation Pressure Instabilities

The resonance condition of the light in the arm cavity depends upon the mirrors' positions and alignment. The mirrors' positions and alignment, in turn, are affected by the light in the cavity through radiation pressure. Above a certain threshold stored power, this cycle becomes unstable. These radiation pressure instabilities are not a problem in LIGO as currently built, although the radiation pressure itself is certainly visible (see Figure 3). In Advanced LIGO, the much higher stored power makes them more of a concern.

The Sidles-Sigg instability¹⁴ is one such radiation pressure effect that is fairly simple to quantify. In a perfectly aligned spherical mirror cavity with cylindrically symmetric mirrors, the stored light exerts no torque on an end mirror, because the mode is incident on the optic on its center of mass. However, if one or both optics are rotated with respect to the cavity axis, the resonant mode structure of the cavity will shift its axis, moving the spots away from the centers of the mirrors, resulting in radiation pressure torque. As Figure 7 shows, this torque will act to restore equilibrium if the mirrors both rotate in the same direction, but will act to further misalign the cavity if the mirrors rotate in opposite directions. For a given cavity geometry, mirror moment of inertia, and mirror stiffness against rotation (determined by the alignment servos), there is a threshold power for which an unstable solution exists, and the cavity alignment can no longer be maintained. Given the desire for a symmetric arm cavity with a spot size of 6 cm, there are two solutions available: a nearly flat cavity, and a nearly concentric cavity. Analysis of the eigenvalues of the stiffness matrix reveal that the Sidles-Sigg threshold power for the nearly concentric cavity is several times larger than that of the flat cavity by a factor of nearly 16, and larger than the design power for Advanced LIGO.

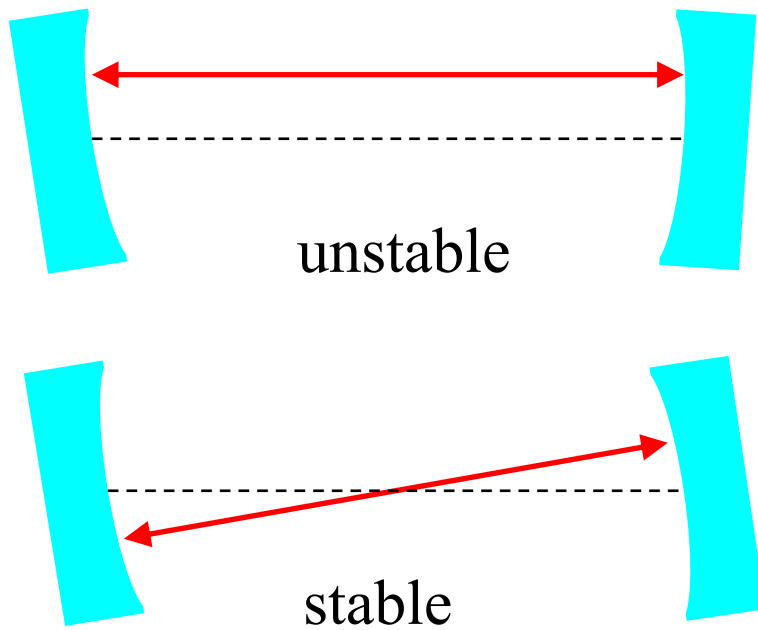


Figure 7: Optical misalignments of arm cavities and the resultant mode axis shifts (red arrows). The dashed line connects the mirrors' centers of mass, making clear the torque imparted by the resonant mode.

The acoustic parametric instability¹⁵ is much more difficult to quantify, and potentially more serious for Advanced LIGO. An arm cavity mirror has acoustic resonant modes which deform its reflective surface, scattering power from the fundamental cavity mode to higher order transverse cavity modes with a frequency shift. The presence of these transverse modes along with the carrier in the cavity leads to an oscillating pressure distribution on the mirror's surface with a spatial profile given by the product of the fundamental and transverse modes. If this oscillating pressure drives the acoustic mode that produced the transverse mode to begin with, then a feedback cycle has been produced which leads to instability above a threshold stored optical power, driving the acoustic mode to higher amplitudes until the cavity can no longer remain locked in resonance. The formula for the parametric gain R of the instability for a single Stokes mode is¹⁶

$$R = \frac{2PQ_m}{McL\omega_m^2} \frac{Q_1\Lambda_1}{1 + \Delta\omega_1^2 / \delta_1^2}$$

This phenomenon is very much like stimulated Brillouin scattering, in that light scatters from an acoustic wave, but is a distinct physical process: the acoustic wave is generated by radiation pressure rather than by electrostriction, and the light scatters from an oscillating surface of an object rather than from refractive gradients within it. The difficulty in predicting the threshold for Advanced LIGO is in predicting the mirrors' acoustic resonant behavior, in particular their mechanical quality factors, and in determining the precise set of transverse optical modes that resonate in the arm cavity with sufficiently low optical losses against diffraction at the mirror edges to build up in the arm cavities. However, the best analysis to date suggests that the instability will be present at Advanced LIGO's design power and must be controlled in some way¹⁶. Several techniques have been proposed¹⁶, including dynamic thermal tuning of the arm cavity mirrors' radii of curvature, active suppression of the acoustic resonances, passive mechanical dissipation added to the mirrors, and feeding transverse mode amplitude into the detector out of phase with the parametrically driven resonances.

2.5. Quantum Noise

Radiation pressure would appear from the above considerations to be a source of nothing but woe to the instrument design. Such is not the case. A careful consideration of the quantum behavior of the coupled optical-mechanical degrees of freedom of the interferometer shows that the radiation pressure can enhance the sensitivity of the instrument in its quantum noise limited regime.

This behavior derives from the addition of the signal recycling mirror to the output of the interferometer. The Michelson interferometer has two ports: input and output. The laser light incident on the input port may be considered to be a classical wave. Due to the operation of the interferometer on a dark fringe, this light recombines upon reflection from the arms and leaves the interferometer back through the input port. The addition of arm cavities and power recycling cavities does not change this basic behavior, but only how much of the light is absorbed in the mirrors. Vacuum electromagnetic fields are incident on the output port. These enter the interferometer, are reflected from the arms, and recombine to exit the interferometer at the output, again due to the operation on a dark fringe. The radiation pressure noise and shot noise of the interferometer can be understood as originated from heterodyning of the two fields in the arms, but these two noises are uncorrelated.

The addition of the signal recycling mirror at the output port causes the vacuum field exiting the interferometer to be fed back into interferometer with 'fresh' vacuum, leading to correlations in the quantum (radiation pressure and shot) noise, and a ponderomotive 'optical spring' acting on the mirror displacement¹⁷. This spring is itself an instability, but one that can be readily suppressed through appropriate design of the length control servomechanisms.

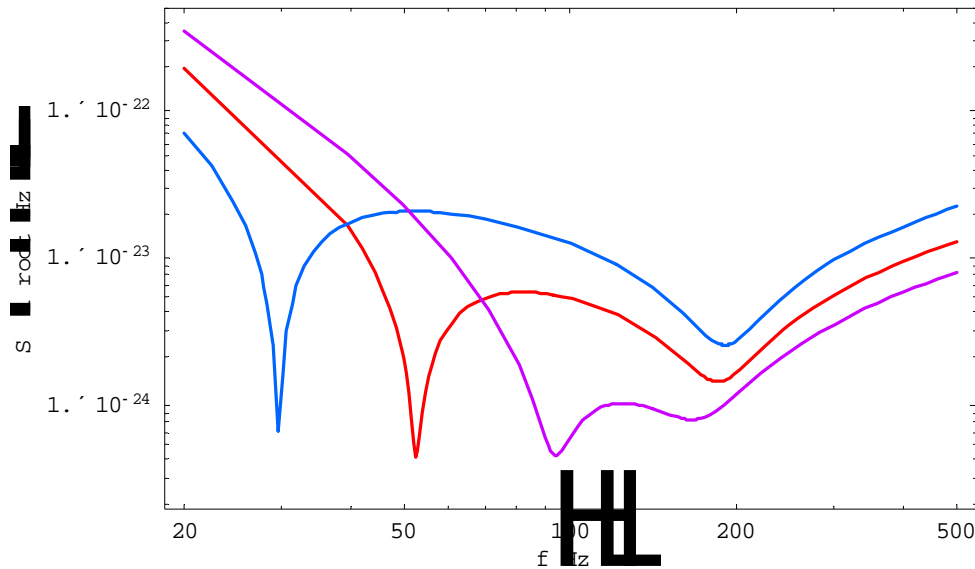


Figure 8: Quantum noise sensitivity curves for Advanced LIGO with 100kW (blue), 300kW (red) and 800kW (violet) arm powers. Adapted from Buonanno and Chen¹⁸.

The optical sensitivity of the interferometer with a detuned signal recycling mirror has the expected sensitivity peak at the frequency for which the coupled arm/signal recycling cavity is resonant (about 200 Hz), but also a sharper peak at lower frequency due to the optical spring. In fact both peaks are solutions to the coupled optomechanical equations of motion for the interferometer, with peak locations that vary with input power: at very low power, the upper peak is precisely at the coupled cavity resonance, while the optical spring peak is nearly at zero frequency; and as the input power increases, the two peaks approach each other in frequency. Because the optical spring is derived from the quantum light field, it does not introduce noise as from a thermal reservoir in the manner of an ordinary mechanical spring, but from the quantum zero-point fluctuations. This makes the optical spring effectively noiseless. Of course, the thermal noise in the interferometer will prevent Advanced LIGO from fully realizing the improvements in sensitivity offered by the optical spring.

ACKNOWLEDGEMENTS

The author acknowledges the LIGO Laboratory and LIGO Science Collaboration for support and review of this work. The original research reported herein was supported by the U.S. National Science Foundation grants PHY-9210038, PHY-0107417, PHY-9801158, and PHY-0098715.

REFERENCES

1. A. Einstein, "Concerning gravitational waves," *Sitzungsberichte der Koniglich Preussischen Akademie der Wissenschaften* Part 1, pp. 154-67, 1918.
2. B. Abbott *et al.*, "Detector description and performance for the first coincidence observations between LIGO and GEO," *Nuclear Instruments and Methods in Physics Research Section A*, pp. 154-79, 2004.
3. P. Fritschel *et al.*, "Readout and control of a power-recycled interferometric gravitational-wave antenna," *Applied Optics* 40, pp. 4988-98, 2001.
4. N. Mavalvala, D. Sigg, and D. Shoemaker, "Experimental test of an alignment-sensing scheme for a gravitational-wave interferometer," *Applied Optics* 37, pp. 7743-6, 1998.
5. LIGO internal document M030023-00M.

6. R. Abbott *et al.*, "Seismic isolation enhancements for initial and Advanced LIGO," *Classical and Quantum Gravity* 21, pp. S915-S921, 2004.
7. N. A. Robertson, "Quadruple suspension design for advanced LIGO," *Classical and Quantum Gravity* 19, pp. 4043-58, 2002.
8. K. A. Strain *et al.*, "Sensing and control in dual-recycling laser interferometer gravitational-wave detectors," *Applied Optics* 42, pp. 1244-56, 2003.
9. E. Khazanov *et al.*, "Compensation of thermally induced modal distortions in Faraday isolators," *IEEE Journal of Quantum Electronics* 40, pp. 1500-10, 2004.
10. E. A. Khazanov *et al.*, "Adaptive compensation of thermally induced aberration in Faraday isolator," in this proceedings.
11. R. Lawrence *et al.*, "Active correction of thermal lensing through external radiative thermal actuation," *Optics Letters* 29, pp. 2635-7, 2004.
12. R. Lawrence, "Active wavefront correction in laser interferometric gravitational wave detectors," Ph.D. thesis, MIT, 2003.
13. V. Zelenogorsky *et al.*, "High-precision methods and devices for *in situ* measurements of thermally induced aberrations in optical elements," in preparation.
14. John A. Sides and Daniel Sigg, "Optical torques in suspended Fabry-Perot interferometers," LIGO document P030055-B-D, 2003.
15. V. B. Braginsky *et al.*, "Analysis of parametric oscillatory instability in power recycled LIGO interferometer," *Physics Letters A* 305, pp. 111-24, 2002.
16. C. Zhao *et al.*, "Parametric instabilities and their control in advanced interferometer gravitational-wave detectors," *Physical Review Letters* 94, art. no. 121102, 2005.
17. A. Buonanno and Y. Chen, "Signal recycled laser-interferometer gravitational-wave detectors as optical springs," *Physical Review D* 65, art. no. 042001, 2002.
18. A. Buonanno and Y. Chen, "Scaling law in signal recycled laser-interferometer gravitational-wave detectors," *Physical Review D* 67, art. no. 062002, 2003.